Available online at www.sciencedirect.com
ScienceDirect
Journal of Power Sources 169 (2007) 288–295
JOURNAL OF POWER SOURCES
www.elsevier.com/locate/jpowsour

XPS investigation of Nafion® membrane degradation

Cheng Chen [a,*], Galit Levitin [a], Dennis W. Hess [a], Thomas F. Fuller [a,b]

[a] *School of Chemical and Biomolecular Engineering, Georgia Institute of Technology, Atlanta, GA 30332, United States*
[b] *Center for Innovative Fuel Cell and Battery Technologies, Georgia Tech Research Institute, Georgia Institute of Technology, Atlanta, GA 30332, United States*

Received 19 January 2007; received in revised form 12 March 2007; accepted 13 March 2007
Available online 18 March 2007

Abstract

After treatment in different Fenton's reagents, chemical changes in Nafion® membranes were analyzed by X-ray photoelectron spectroscopy (XPS) and clear evidence of polymer degradation was observed. Exposure of the membrane to 2 h of X-ray radiation did not affect the chemical structure of the membrane. However, treatment with various Fenton's reagents indicated that the $(CF_2)_n$ polymer backbone had decomposed. Fluorine and sulfur XPS peak intensity decreases were consistent with the detection of fluoride and sulfate ions during fuel-cell tests. The increase in oxygen atom concentration suggests that oxygen-rich moieties formed in the membrane. These results indicated that in addition to degradation of the polymer side chain, chemical attack of the CF_2 backbone may be the primary reason for extensive fluorine loss and hydrogen crossover in membranes after long-term operation. FTIR spectra showed the formation of C=O and S–O–S in the degraded membrane. Two degradation schemes consistent with the results observed have been proposed. Under the same experimental conditions, no detectable changes in XPS spectra were found between a fresh membrane electrode assembly (MEA) and an MEA after long-term operation. These results suggest that degradation occurred mainly within the membrane or at the membrane-electrode interface.

Keywords: Membrane degradation; Nafion®; Membrane electrode assembly; X-ray photoelectron spectroscopy; Fourier transform infrared spectroscopy; Fenton's test

1. Introduction

Nafion® membranes display chemical stability, permselectivity and high proton conductivity; as a result, since their appearance in the mid-1960s [1], they have been widely used as proton exchange membranes. Although Nafion® perfluorosulfonic acid (PFSA) polymer has demonstrated high efficiency and stable performance in fuel-cell applications, evidence of polymer degradation is detected after a few hundred to a few thousand hours depending upon the operating conditions [2–4]. It is believed that membrane degradation is mainly caused by chemical attack of the polymer [2,5]. Previous work has suggested that hydroxyl free radicals, generated from homolytic cleavage of H_2O_2 catalyzed by metal impurities, can attack polymer end groups having H-containing terminal bonds (such as $-CF_2COOH$) that are formed during membrane processing [2]. Indeed, carbon radicals in the electrode and unspecified radical centers in the membrane have been identified previously in a PEM fuel cell using electron spin resonance (ESR) [6,7].

X-ray photoelectron spectroscopy (XPS) has been used previously to study chemical changes in the polymer membrane. For instance, Schulze et al. used XPS to study the degradation of Nafion® under X-ray exposure [8,9] and reported that changes in both the PTFE backbone and the side chain occurred. XPS analysis of fresh and degraded membrane electrode assemblies (MEAs) was carried out by Huang et al. [10] XPS measurements revealed that Nafion® decomposed after fuel-cell operation, particularly in the hydrogen potential region of the cell. Therefore, it is likely that under the anode potential, the hydrophobic part (i.e., fluorocarbon) in the Nafion® electrolyte may react with carbon or hydrogen atoms, yielding –HCF– or –CCF– configurations which ultimately result in degradation of the electrolyte.

Membrane degradation during fuel-cell operation is believed to be due to the formation of hydrogen peroxide caused by

* Corresponding author. Tel.: +1 404 894 2834; fax: +1 404 894 2291.
E-mail address: cheng.chen@chbe.gatech.edu (C. Chen).

0378-7753/$ – see front matter © 2007 Elsevier B.V. All rights reserved.
doi:10.1016/j.jpowsour.2007.03.037

diffusion of oxygen across the membrane where it reacts with hydrogen. Data from W. Liu and D. Zuckerbrod [11] show that H_2O_2 formation is inversely proportional to membrane thickness. Therefore, the rate of chemical degradation of the membrane will depend upon the rate of gas crossover. For example, H_2 and O_2 permeability across an MEA with Nafion® 111 membrane are reported to be 1.61×10^{-8} and 1.3×10^{-9} mol $(cm^2\ s)^{-1}$, respectively [12]. After achieving steady state, we can assume that O_2 and H_2 crossover will be constant under a fixed O_2 partial pressure. Normally, cell potential is not expected to change significantly, so the generation of peroxide should also be nearly constant. Under these conditions, the membrane degradation rate is determined solely by the level of metal ion contaminants such as Fe^{2+} and Cu^{2+}.

Fenton's reagent is a well-known source of hydroxyl radicals, and the similarity between the *in situ* (fuel-cell operation) and *ex situ* (Fenton's test) degradation mechanism has been reported [13]. However, performance of a membrane in such a test is not necessarily a good prediction of its durability under fuel-cell conditions. Recently developed non-fluorinated membranes such as 4,4′-biphenol based poly(arylene ether sulfone) copolymers [14] have been reported to degrade extensively in Fenton's test but demonstrate longer lifetimes than do Nafion® membranes in open circuit voltage (OCV) tests due to low O_2 permeability. Therefore, our objective in this study is to use *ex situ* tests to demonstrate the ability of XPS to identify chemical changes in the membrane that can be related to both the relative concentration of hydrogen peroxide and fuel cell operating conditions. Since the level of metal contaminants and peroxide concentration are easier to control with Fenton's test compared to fuel-cell durability tests, we first use XPS to analyze membranes exposed to Fenton's test before considering analyses of membranes that have been exposed to fuel-cell conditions. In order to accelerate membrane degradation, the Fe^{2+} concentrations in Fenton's reagent are varied from 3 ppm to 300 ppm. Clearly, Fenton's test yields much more aggressive reaction conditions than those encountered in the fuel cell, where the metal contaminant level is likely to be on the order of 1 ppm according to the NEDO report from Mitsuda [15]. Degradation data are collected and the membrane samples are analyzed by XPS after Fenton's test; FTIR is also invoked to validate the XPS results. The effects of Fe^{2+} concentration and temperature on membrane degradation are discussed. After fuel-cell durability tests, the degraded MEA is also analyzed and results are compared with those on a fresh MEA. To the authors' knowledge, this is the first application of XPS to correlate surface analysis and degradation studies of Nafion® membranes. The experimental results provide evidence of chemical attack of the CF_2 backbone.

2. Experimental

2.1. Ex situ Fenton's test

Nafion® 112 (Dupont), with a thickness of 51 μm and an equivalent weight of 1100, was used for all experiments. XPS analyses demonstrated that the Nafion® membrane consists of approximately 31.5 atom% carbon, 58.8% fluorine, 8.4% oxygen and 1.3% sulfur, which is consistent with previous XPS studies [8]. Ferrous sulfate with 7-hydrate (A.C.S. grade, from J.T. Baker Chemical Co.) was dissolved into an aqueous solution of hydrogen peroxide (A.C.S. grade, from Fisher Scientific) to prepare Fenton's reagent. Because the ferrous ion accelerates H_2O_2 decomposition to generate O_2, fresh Fenton's reagent was used in each experiment.

The *ex situ* Fenton's test included the following steps:

Membrane pretreatment: First the membrane was treated with a 2% solution of hydrogen peroxide at 80 °C and rinsed in boiling de-ionized water for 0.5 h. Then the membrane was heated in 0.5 M sulfuric acid for 0.5 h at 80 °C to remove metallic impurities. Subsequently, the membrane was repeatedly washed with de-ionized water at the same temperature for 1 h to remove sulfuric acid and then dried in air.

Fenton's test: Fenton's test was conducted using 10% (wt) hydrogen peroxide and different concentrations of iron salts. The membrane was weighed and placed in a wide mouth bottle. One hundred milliliters of H_2O_2 solution with the appropriate amount of Fe^{2+} were added to the solution. Then the membrane was treated in the Fenton's reagent at 80 °C for several hours. After treatment, it was repeatedly washed with 80 °C deionized water and dried by carefully pressing between two filter papers. The resulting solution was analyzed for fluoride ion content using an ICS-2000 Ion Chromatography System (Dionex Corporation). The fluoride ion peak at approximately 3.2 min is the first anion to elute and was quantified using a calibration curve generated with fluoride standards (Ricca Chemical).

2.2. XPS (X-ray photoelectron spectroscopy)

Chemical analysis of Nafion® membranes and MEA samples were performed by XPS. The spectra were collected using a Physical Electronics (PHI) Model 1600 XPS system equipped with a monochromator and an Al Kα source ($h\nu = 1486.8$ eV) operating at 350 W beam power. Ejected photoelectrons were detected by a hemispherical analyzer that provided both high sensitivity and resolution. The operating pressure in the sampling chamber was below 5×10^{-9} Torr. Samples were aligned in the beam by maximizing photoelectron counts corresponding to the primary C 1s peak in C–C bonds located at a binding energy of 284.8 eV. A neutralizer beam was used during XPS measurements to compensate for peak shifting that occurs due to charging of samples during X-ray exposure. All high resolution spectra were collected using a pass energy of 46.95 eV. The step size and time per step were chosen to be 0.025 eV and 100 ms, respectively. Atomic concentrations of different elements were calculated based on the photoelectron intensities of each element and the elemental sensitivity factors provided by PHI. Samples were scanned at different locations and the peak intensity and composition at different locations were compared to assure uniformity of film composition over the sample surface.

2.3. FTIR (Fourier transform infrared spectroscopy)

FTIR spectra were collected on a Bruker IFs66vS FTIR system with KBr as a beam splitter. Spectra, collected as the average

Table 1
XPS results for different samples in Fenton's test (H_2O_2 concentration is fixed at 10 wt.%)

	Treatment conditions			Element composition in atom%				
	Fe^{2+} concentration (ppm)	Temperature (°C)	Time (h)	Carbon	Oxygen	Sulfur	Fluorine	Impurities
Pretreated	–	80	–	31.5	8.4	1.3	58.8	–
Sample 1	300	80	24	20.2	53.1	1.4	5.8	19.5
Sample 2	30	80	24	27.8	36.6	0.9	21.3	13.4
Sample 3	3	80	24	29.7	19.5	1.4	44.7	4.7
Sample 4	30	60	8	32.4	8.7	1.3	57.7	–

of 128 scans with a resolution of 4 cm^{-1}, were recorded from 4000 to 400 cm^{-1} in absorption mode.

2.4. In situ durability test

5 cm × 5 cm membrane electrode assemblies (MEAs) covered with gas diffusion layers (GDLs) were supplied by a commercial vendor. The MEA included Nafion® 111 membrane and Pt/C catalyst layers with Pt loadings of 0.3 and 0.5 $mg_{Pt}\,cm^{-2}$ in the anode and cathode respectively. MEA with Nafion® 111 membrane is more prone to chemical attack because of higher oxygen crossover. However, in the *ex situ* Fenton's test, the membrane thickness is not relevant since oxygen crossover is not needed to form H_2O_2. The MEA and GDL were assembled in 25 cm^2 fuel-cell testing hardware (Fuel Cell Technologies, Inc.). Long-term fuel-cell durability tests were conducted on the Fuel Cell Test Station (Teledyne Energy System Inc. Model 890CL). The cell operating conditions were: open circuit voltage ~0.9 V, $T = 65\,°C$, RH = 30%, H_2 flow rate = 0.1 L min^{-1}, Air flow rate = 0.3 L min^{-1}, and atmospheric pressure. Water was collected from both the anode and cathode. Fluoride ion concentration in the exhaust water was measured by ion chromatography and the fluoride ion emission rate (FER) was determined every 24 h.

3. Results and discussion

3.1. Effect of Fe^{2+} concentration on membrane degradation

Nafion® membrane samples were exposed to Fe^{2+} concentrations of 3, 30 and 300 ppm (corresponding to samples 3, 2 and 1, respectively) and a constant H_2O_2 concentration of 10 wt.% at 80 °C for 24 h. To investigate the effect of time and solution temperature, an additional membrane sample was exposed to 30 ppm Fe^{2+} (sample 4) at 60 °C for 8 h (Table 1).

Fig. 1 shows the effect of Fe^{2+} concentration on membrane degradation. It is interesting to note that the highest Fe^{2+} concentration corresponds to lowest FER, which is consistent with the results from Kodama et al. [16]. However, Schiraldi [17] has pointed out that literature reports that show surprisingly low FER under aggressive Fenton's test may be in error due to the existence of Fe^{3+} in Fenton's reagent when using commercial ion-selective electrodes. In the current study, we avoided this error by using ion chromatography to measure fluoride ion content. More likely, the decrease in FER is due to different degradation products under different Fe^{2+} concentrations. At low Fe^{2+} concentrations, the main degradation product would be fluoride ion and a very small number of polymer fragments in this mild environment. As the Fe^{2+} concentration increases, the radicals may attack less active bonds such as C–O in the polymer. For example, Healy et al. [13] found a degradation product in a Fenton's test bath water with the structure HOOC–$CF(CF_3)$–O–CF_2–CF_2–SO_3H. Therefore, polymer fragments may have been a dominant degradation product, but are not detectable by ion chromatography. Although the XPS spectra discussed below show a large loss of fluorine from the membrane after Fenton's test with the highest Fe^{2+} concentration, the low F^- emission rate cannot account for this large loss. Nevertheless, Fenton's test under aggressive conditions may provide sufficient degradation products for further study by NMR and mass spectroscopy; these studies are underway in our laboratory.

3.2. Effect of temperature on membrane degradation

Fig. 2 shows membrane degradation rates at different temperatures for the Fenton's test. Clearly, degradation rates increase with temperature; FER increased by approximately a factor of 2 after a temperature increase of 10 °C. These results suggest that the lifetime of Nafion® membranes will be greatly diminished when operating above 100 °C. Therefore, identifying the membrane degradation mechanism is crucial to the improvement of membrane durability and can serve as a guide to the development of novel high temperature membranes.

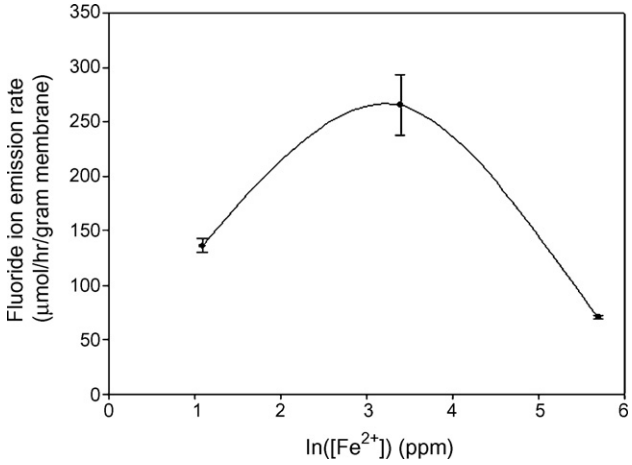

Fig. 1. Effect of Fe^{2+} concentration on membrane degradation.

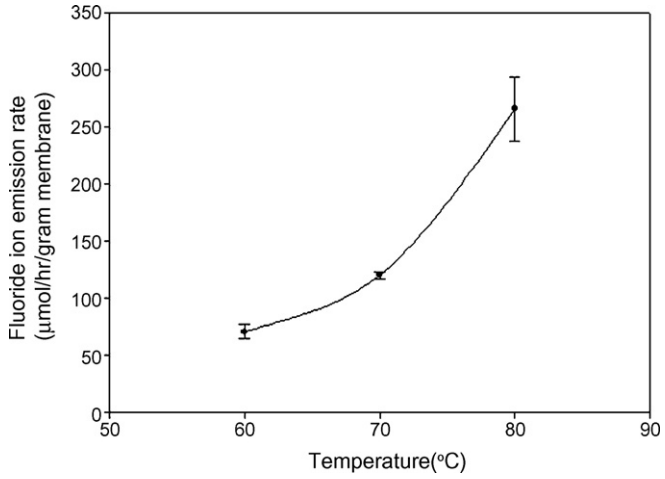

Fig. 2. Degradation rates under different temperatures (Fe^{2+} fixed at 30 ppm).

3.3. X-ray radiation effect on membrane degradation

Pretreated Nafion® membrane samples were exposed to X-ray radiation in the XPS chamber and XPS spectra were recorded (Fig. 3) as a function of exposure time. X-ray radiation did not cause a discernable change in the chemical structure of the membrane, even after 2 h of exposure. Since the typical XPS analysis time for these membranes is only ~20 min, these results demonstrate that there is a sufficient time window to allow XPS analysis of membrane degradation resulting from electrochemical activity without introducing additional changes due to radiation exposure.

3.4. XPS analyses of the membranes

Fig. 4(a) shows the C 1s spectra of different membrane samples. For carbon in the CF_2 configuration, the binding energy (E_b) is ~291 eV (highest binding energy peak). The XPS peak at E_b = 284.2 eV can be related to the carbon in C–CF or C–C configuration. It is apparent that the intensity of the peak at 291 eV decreases when the Fe^{2+} concentration is increased; after treatment with the 300 ppm Fe^{2+} solution, this peak is nearly undetectable, indicating that the $(CF_2)_n$ polymer backbone has decomposed. However, the intensity of the peak at 284.2 eV for samples 2 and 3 has increased, indicating that the relative concentrations of C–C or C–CF configurations have increased with increasing Fe^{2+}.

These results demonstrate that fluorine atoms are removed from the CF_2 bonding configuration to form fluorine depleted configurations as a result of treatment with Fenton's reagent. For the highest Fe^{2+} concentration (sample 1), the CF_2 intensity decreased and the binding energy shifted to lower values. Such observations are consistent with a removal of fluorine atoms, resulting in a reduced binding energy for C 1s.

Fig. 4(b) shows the O 1s spectrum for different membrane samples. Oxygen in Nafion® membranes has two different

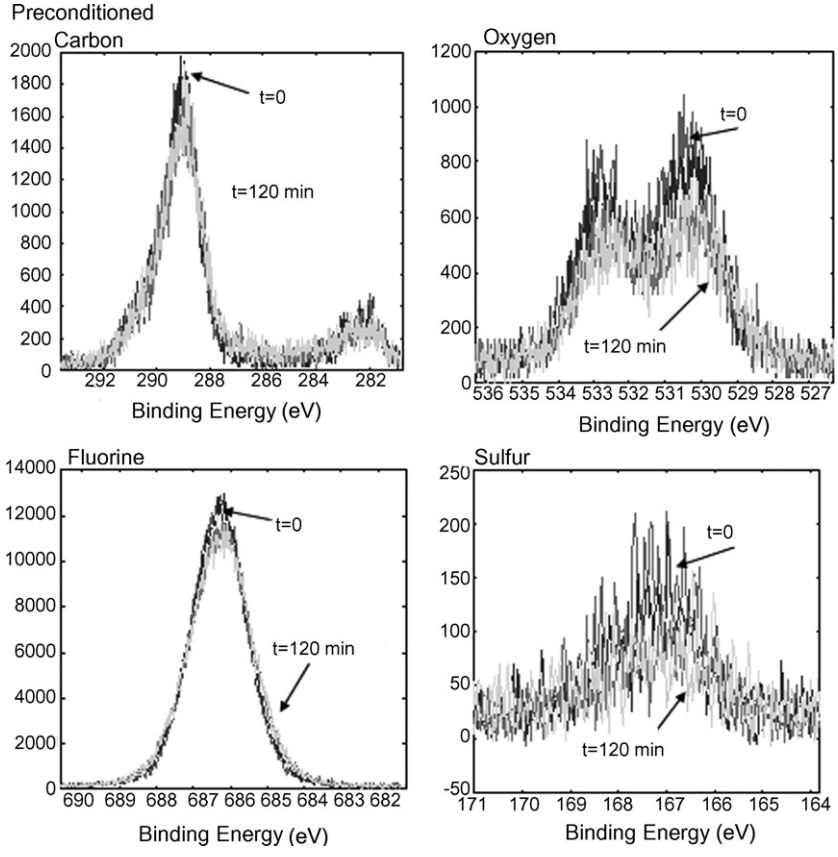

Fig. 3. XPS spectra changes with X-ray exposure time.

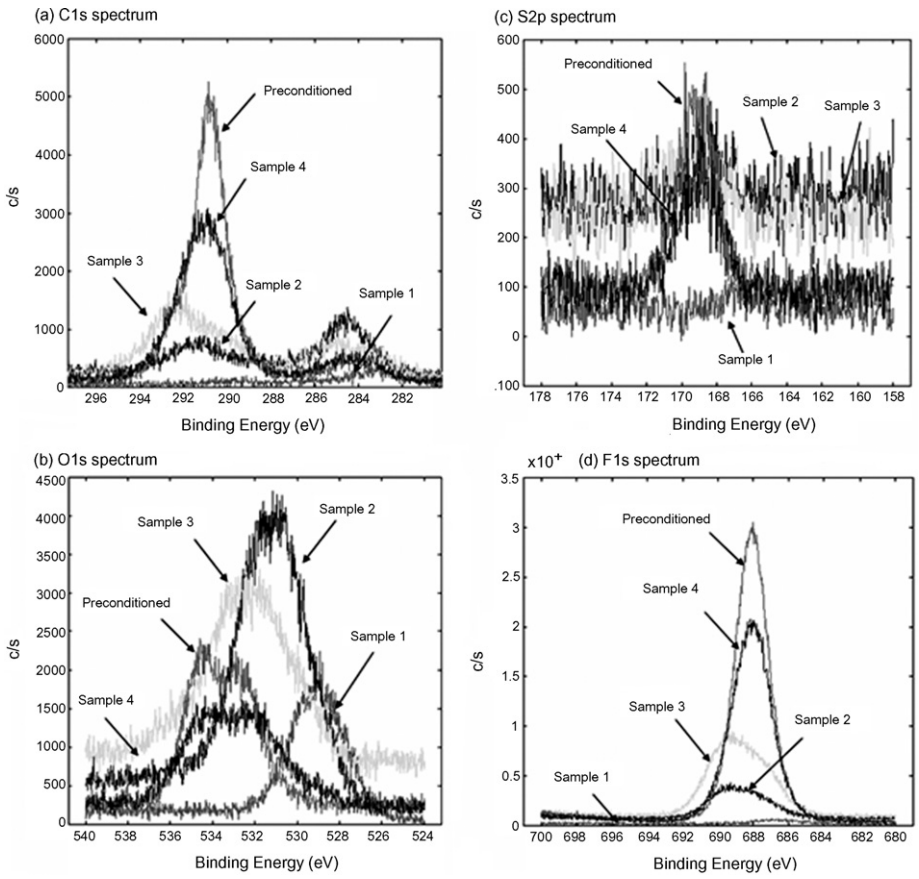

Fig. 4. XPS spectra of different membrane samples.

binding states. Three oxygen atoms are bound in each sulfonic acid group, indicated by $E_b = 535.7$ eV (highest binding energy peak). Two of the oxygen atoms in the polymer chain are in ether configurations with $E_b = 533$ eV (lower binding energy peak). After treatment of samples 1–3 (Table 1) in Fenton's reagent, only the ether bonding configuration is observed. Furthermore, with an increase in Fe^{2+} concentration, the oxygen binding energy is shifted to lower values. This shift is consistent with the formation of an oxo-bonded iron complex on the membrane surface [18,19] along with the loss of $–SO_3H$ groups from the membrane. Such results also agree with the detection of SO_4^{2-} in the exhaust water by ion chromatography.

Fig. 4(c) shows the S 2p spectrum for different membrane samples; S 2p electrons have a binding energy of 168 eV. The binding energy of sulfur does not change after exposure to Fenton's reagent, but the signal intensity decreases, indicating a loss of sulfur from the polymer. Such observations and conclusions are consistent with the changes observed in the O 1s spectrum and the detection of SO_4^{2-} in the effluent [20].

Fig. 4(d) shows the F 1s spectrum for different membrane samples; F 1s electrons have a binding energy of 688 eV. A substantial decrease in peak intensity has occurred as a result of the Fenton's reagent treatment. In fact, for the highest Fe^{2+} concentration (sample 1), the fluorine signal is weak, indicating a low fluorine atomic percentage (Fig. 4(d) and Table 1).

3.5. Atomic percentage data analyses

Table 1 gives the treatment conditions and quantitative (peak fitting) XPS results for various samples that were exposed to Fenton's reagent. Limited changes in elemental concentrations were observed after Fenton's test at 60 °C (sample 4). These results are consistent with the FER data from Fig. 2, which shows that the FER at 80 °C is three times larger than that at 60 °C. Such observations are expected, since the polymer degradation rate should be reduced at lower temperatures.

The oxygen concentration in the polymer increases during each test, whereas the sulfur concentration remains low. This result indicates that most of the oxygen atoms are not bonded to sulfur. Two plausible reasons for the increase in oxygen concentration can be offered. First, the main contribution is likely due to the oxo-bonded iron complex. Since the hydrophilic sulfonic acid group in the side chain can move from the membrane bulk to the surface during treatment [8], the oxo-bonded iron complex can form after a proton in $–SO_3H$ is exchanged with a ferric ion in Fenton's reagent [18]. However, the oxygen concentration in the polymer still increases even after subtracting the maximum number of oxygen atoms bonded to iron (in the form of Fe–OOH). Second, although carbon and fluorine are removed as a result of chemical attack and replaced by oxygen, there is also considerable oxygen loss from the removal of $–SO_3H$ groups. Therefore, loss of carbon and fluorine is probably not

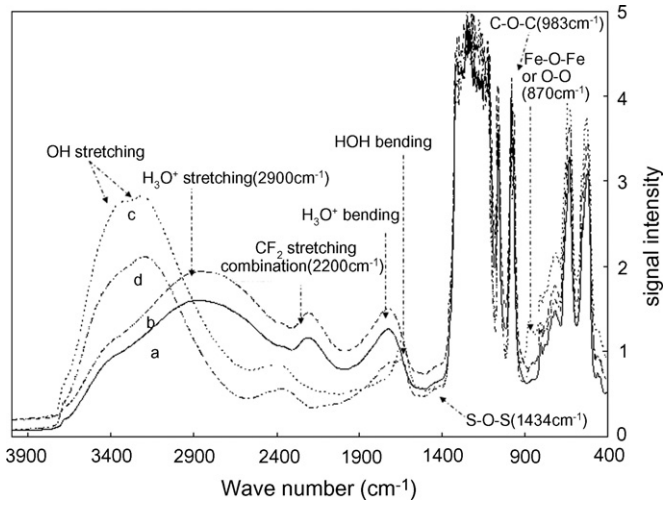

Fig. 5. FTIR spectra of initial, pretreated and tested membrane samples: a (——) initial membrane sample, b (- - - - -) pretreated membrane sample, c (· · · · · · · · · · · ·) 300 ppm Fe^{3+} treated membrane sample, d (- · - · -) 3 ppm Fe^{3+} treated membrane sample.

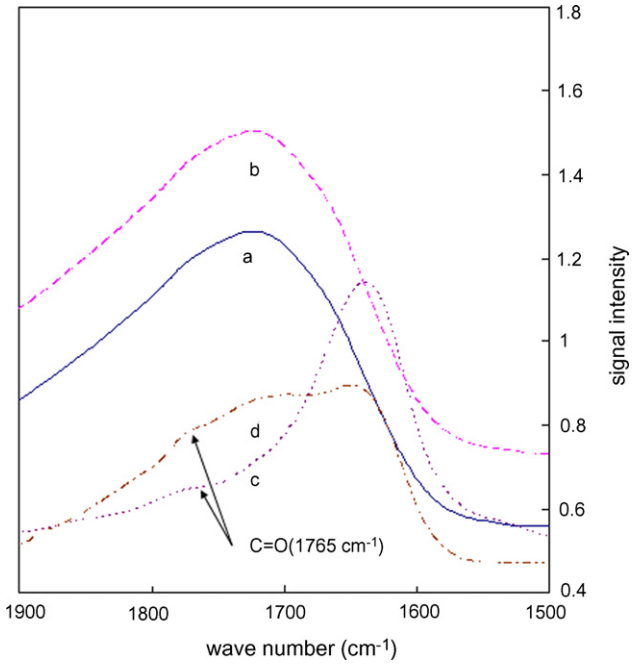

Fig. 6. FTIR spectra of membrane samples in 1900 cm^{-1} and 1500 cm^{-1} short range: a (——) initial membrane sample, b (- - - -) pretreated membrane sample, c (· · · · · · · · · · · ·) 300 ppm Fe^{3+} treated membrane sample, d (- · - · -) 3 ppm Fe^{3+} treated membrane sample.

the dominant reason for the increase in oxygen concentration in the polymer. The most probable source of oxygen is from the hydroxyl free radical (•OH). Attack of the polymer chain by this radical forms O–O or C=O moieties. The atomic ratio of carbon to oxygen drops after each test. The high oxygen content relative to carbon suggests the formation of polymeric species that contain large amounts of oxygen. That is, one result of chemical attack of the polymer chain may be the formation of peroxide or carbonyl groups in the degraded membrane.

3.6. FTIR studies of the membrane

In order to verify XPS results, FTIR was used to study the chemical structure of Nafion® membranes before and after Fenton's test. Fig. 5 shows the FTIR spectra of initial, pretreated, 3 ppm Fe^{2+} treated and 300 ppm Fe^{2+} treated (both with 10% H_2O_2) membrane samples. Spectra of initial and pretreated Nafion® membranes are consistent with observations on Nafion® membranes reported previously [21,22]. The broad absorption between 3700 and 2900 cm^{-1} is assigned to the fundamental stretching vibration of water. A shift of this band from 2900 cm^{-1} to 3200 cm^{-1} is observed in the tested membrane. This shift results from the fact that the band at 2900 cm^{-1} can also be assigned to the stretching band of H_3O^+ [21]. That is, after Fenton's test, some of the protons attached to sulfonic groups have been exchanged with Fe^{2+} or Fe^{3+}, thereby decreasing the H_3O^+ content in the membrane and resulting in a peak shift. This conclusion is consistent with the disappearance of the band at 1710 cm^{-1} in the degraded membrane, which corresponds to the H_3O^+ asymmetric bending mode [21]. The band at 2200 cm^{-1} is assigned to the CF_2 stretching combination [23,24]. A shift to higher wave number accompanied by an intensity decrease was observed for tested membranes, which demonstrated a loss of CF_2 groups in the degraded membrane and is consistent with XPS spectra. The band at 1630 cm^{-1} is assigned to the HOH fundamental bending mode [21,24].

It should be noticed that on the high wavenumber shoulder of this peak a weak but broad band appears; this spectral region is enlarged in Fig. 6. The band at 1765 cm^{-1} may be assigned to the carbonyl bond in esters or carboxylic acids. Such observations offer evidence of the formation of oxygen-rich groups such as esters or carboxylic acid groups, which is in agreement with XPS results. A very weak absorption at 1434 cm^{-1} is also evident; this peak has been assigned to a cross-linking S–O–S band by J. Qiao et al. [25] This assignment can be further verified by the fact that two water bands appear in the range 3000–4000 cm^{-1}. In the previous degradation [25] study using H_2O_2, these peaks were not observed until the membrane was exposed to H_2O_2 for 3 weeks; this can be compared to 24 h of exposure to Fenton's test in our study. Such observations indicate that free radicals will aggressively attack the membrane and lead to the loss of sulfonic groups which may cause performance decay in fuel-cell tests. Another absorption detected is the band at 870 cm^{-1}, which can be assigned to oxo-bonded Fe–O–Fe in Fe^{3+}-Nafion [18]. However, since the O–O stretch in Nafion® has also been reported [26] to be in this narrow range (845–875 cm^{-1}), this peak could be due to O–O, or to a combination of O–O and Fe–O–Fe bands.

3.7. Degradation mechanism

Based on the experimental results provided above, the degradation mechanism of Nafion® can be considered to occur via two schemes. The first scheme occurs due to the attack of defects in the main chain such as "residual" C–H bonds that have been reported to exist in the Nafion® polymer [27]. It is well-known that carbon-fluorine bonds are strong (~460 kJ mol^{-1}) com-

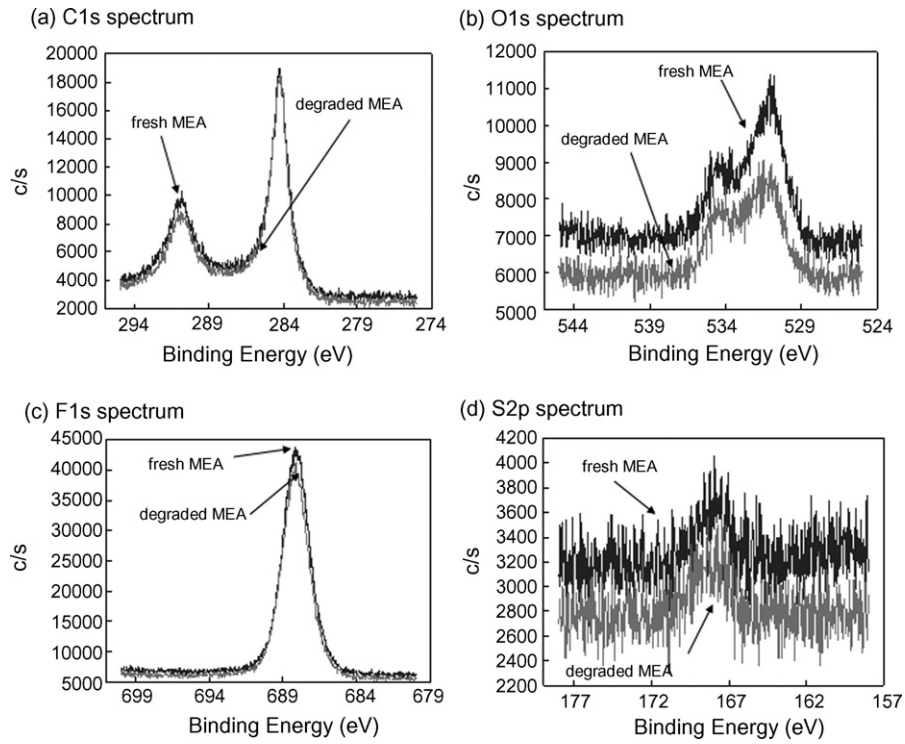

Fig. 7. XPS spectra of fresh and degraded MEAs.

pared to carbon–hydrogen bonds (~410 kJ mol^{-1}) [5]. In fact, C–F bonds are responsible for the chemical stability of Nafion® membranes, and are thus unlikely to be attacked extensively by free radicals. However, defects such as C–H or C=C bonds, which may form in the polymer during the manufacturing process, are sufficient to initiate radical reactions and eventually degrade Nafion® [27]. These defects can be attacked by hydroxyl or hydroperoxy radicals to form carbon-centered radicals, which have been observed by EPR studies [6,28]. The carbon-centered radical is not stable; thus, it can undergo further radical reaction with hydroxyl radicals or even O_2 and water to generate more stable peroxyl radicals or ester structures and thereby produce fluoride ions and polymer fragments. This process can lead to the cleavage of polymer chains, which is referred to "decomposition of $(CF_2)_n$ polymer backbone". Another degradation scheme is associated with the end group $–SO_3H$, the first step of which is the formation of cross-linking S–O–S bonds under the strong oxidation effect of H_2O_2 and free radicals. This anhydride may react with another sulfonic acid group to produce a sulfonate ester and release SO_2 gas, which has been detected in the exhaust gas of fuel cells by direct gas mass spectroscopy (DGMS) [29]. Reaction of this ester with water produces a carboxylic acid that can be further attacked by hydroxyl radicals. This reaction of the $–SO_3H$ group may account in part for the non-zero intercept in plots of fluoride generation rate versus carboxylic acid content in Nafion® [17]. That is, the sulfonic acid end group could be an additional point of attack by peroxide after transformation into a carboxylic acid end group occurs via the above scheme. Moreover, S. Hommura et al. reported that the carboxylic acid content in the membrane increased during OCV tests [30], which also indicates the possibility of –COOH formation from $–SO_3H$ groups. This scheme is analogous to one of the degradation schemes reported for Nafion® during thermal degradation [31]. However, it should be stressed that this process is kinetically very slow under fuel-cell conditions compared to the degradation of carboxylic acid end groups; as a result, this mechanism may explain the observed continuous fluoride ion emission during the fuel-cell lifetime.

3.8. XPS spectra of the MEA (membrane electrode assembly)

Fig. 7(a)–(d) shows XPS spectra of the electrode surface of both fresh and degraded MEA. Because the electron mean free path in solids is <10 nm, XPS samples only near surface regions, and thus yields chemical information regarding the electrode surface, which contains Pt catalyst and Nafion ionomers. No significant difference between the structure of fresh and degraded MEA was found by XPS. However, analysis of the water collected from the anode and cathode regions showed that ~8.4% of the total fluorine was lost after 236 h of operation. Such results suggest that the Pt catalyst in the electrode may help to protect Nafion ionomers from degradation [32]. If this is correct, the degradation may occur primarily within the membrane or in the electrode but near the membrane interface.

4. Conclusions

Fenton's tests on Nafion® membranes demonstrate the effects of Fe^{2+} concentration and temperature on membrane degradation. Under various Fe^{2+} concentrations, different degradation products were generated. With increasing Fe^{2+} concentrations,

the fraction of degradation products that are polymer fragments increase. Furthermore, membrane degradation is accelerated at high temperatures. After pretreatment and Fenton's test, Nafion® membrane samples were analyzed by XPS to investigate chemical changes in the polymer. Results indicate that X-ray radiation has little effect on membrane degradation even up to 2 h of exposure. These observations confirm that changes in XPS spectra of treated membranes give an indication of chemical bonding and composition changes resulting from treatment with Fenton's reagent. Carbon XPS studies of membranes after treatment show an intensity decrease in the bonding peak related to the CF_2 configuration. Analyses of the O 1s spectra suggest that the oxygen present after treatment is primarily in the ether configuration or bonded with iron, since $–SO_3H$ groups have been diminished. The loss of fluorine and sulfur as indicated by S 2p and F 1s XPS spectra is consistent with the detection of F^- and SO_4^{2-} in exhaust water from MEAs during fuel-cell operation. Oxygen atom analyses indicate that chemical groups with a high carbon to oxygen ratio are generated in the membrane, apparently due to free radical attack of the polymer backbone by $^{\bullet}OH$. FTIR studies verified the formation of oxygen-rich moieties in the degraded membrane, since C=O and O–O bands were evident in the spectra. Moreover, formation of cross-linking S–O–S was observed which can initiate further degradation by producing carboxylic acid groups. Two membrane degradation schemes have been proposed: degradation initiated by polymer defects and by cross-linking of sulfonic end groups. No significant difference between fresh and degraded MEAs is found in the XPS spectra, indicating that membrane degradation likely occurs at the electrode–membrane interface or within the membrane bulk. Further XPS and FTIR analyses, including depth profiling of the membrane separated from MEA is therefore required to obtain additional insight into the membrane degradation mechanism.

Acknowledgements

In part, this research has been supported by the Assistant Secretary for Energy Efficiency and Renewable Energy, Office of Hydrogen, Fuel Cell, and Infrastructure Technologies, of the U.S. Department of Energy under contract number DE-AC02-05CH11231 through a subcontract from Lawrence Berkeley National Laboratory. The authors thank Mr. Wu Bi, Mr. Kevin Gallagher and Ms. Rajeswari Chandrasekaran for helpful discussions.

References

[1] W.G. Grott, Macromol. Symp. 82 (1994) 161.
[2] D.E. Curtin, R.D. Lousenberg, T.J. Henry, P.C. Tangeman, M.E. Tisack, J. Power Sources 131 (2004) 41.
[3] E. Endoh, S. Terazono, H. Widjaja, Y. Takimoto, Electrochem. Solid-State Lett. 7 (2004) A209.
[4] S.D. Knights, K.M. Colbow, J. St-Pierre, D.P. Wilkinson, J. Power Sources 127 (2004) 127.
[5] M. Pianca, E. Barchiesi, G. Esposto, S. Radice, J. Fluorine Chem. 95 (1999) 71.
[6] A. Panchenko, H. Dilger, E. Möller, T. Sixt, E. Roduner, J. Power Sources 127 (2004) 325.
[7] G. Hubner, E. Roduner, J. Mater. Chem. 9 (1999) 409.
[8] M. Schulze, K. Bolwin, E. Gulzow, W. Schnurnberger, Fresenius J. Anal. Chem. 365 (1999) 106.
[9] M. Schulze, M. Lorenz, N. Wagner, E. Gulzow, Fresenius J. Anal. Chem. 353 (1995) 778.
[10] C. Huang, K.S. Tan, J. Lin, K.L. Tan, Chem. Phys. Lett. 371 (2003) 80.
[11] W. Liu, D. Zuckerbrod, J. Electrochem. Soc. 152 (2005) A1165.
[12] W. Bi, G. Gray, T. Fuller, Electrochem. Solid-State Lett. 10 (2007) B101.
[13] J. Healy, C. Hayden, T. Xie, K. Olson, R. Waldo, M. Brundage, H. Gasteiger, J. Abbott, Fuel Cells 5 (2005) 302.
[14] F. Wang, M. Hichner, Y. Kim, T. Zawodzinski, J. McGrath, J. Membr. Sci. 197 (2002) 231.
[15] K. Mitsuda, NEDO Rep., FY. 1996, 1997, p. 90.
[16] K. Kodama, F. Miura, N. Hasegawa, M. Kawasumi, Y. Morimoto, Proceedings of the 208th Meeting of the Electrochemical Society - Meeting Abstracts, 2005, p. 1185.
[17] D.A. Schiraldi, J. Macromol. Sci., Part C: Polym. Rev. 46 (2006) 315.
[18] J. Kiwi, N. Denisov, Y. Gak, N. Ovanesyan, P. Buffat, E. Suvorova, F. Gostev, A. Titov, O. Sarkisov, P. Albers, V. Nadtochenko, Langmuir 18 (2002) 9054.
[19] S. Parra, I. Guasaquillo, O. Enea, E. Mielczarski, J. Mielczarki, P. Albers, L. Kiwi-Minsker, J. Kiwi, J. Phys. Chem. B 107 (2003) 7026.
[20] T. Kinumoto, M. Inaba, Y. Nakayama, K. Ogata, R. Umebayashi, A. Tasaka, Y. Iriyama, T. Abe, Z. Ogumi, J. Power Sources 158 (2006) 1222.
[21] M. Laporta, M. Pegoraro, L. Zanderighi, Phys. Chem. Chem. Phys. 1 (1999) 4619.
[22] A. Gruger, A. Regis, T. Schmatko, P. Colomban, Vib. Spectrosc. 26 (2001) 215.
[23] R. Iwamoto, K. Oguro, M. Sato, Y. Iseki, J. Phys. Chem. B 106 (2002) 6973.
[24] Y. Wang, Y. Kawano, S. Aubuchon, R. Palmer, Macromolecules 36 (2003) 1138.
[25] J. Qiao, M. Saito, K. Hayamizu, T. Okada, J. Electrochem. Soc. 153 (2006) A967.
[26] V. Vacque, B. Sombret, J. Huvenne, P. Legrand, S. Suc, Spectrochim. Acta Part A 53 (1997) 55.
[27] A. Alentiev, J. Kostina, G. Bondarenko, Desalination 200 (2006) 32.
[28] A. Bosnjakovic, S. Schlick, J. Phys. Chem. B 108 (2004) 4332.
[29] K. Teranishi, K. Kawata, S. Tsushima, S. Hirai, Electrochem. Solid-State Lett. 9 (2006) A475.
[30] S. Hommura, K. Kawahara, T. Shimohira, Proceedings of the 207th Meeting of the Electrochemical Society - Meeting Abstracts, 2005, p. 803.
[31] C. Wilkie, J. Thomsen, M. Mittleman, J. Appl. Polym. Sci. 42 (1991) 901.
[32] M. Aoki, H. Uchida, M. Watanabe, Electrochem. Commun. 8 (2006) 1513.